High-voltage Step-up Ratio Single-phase Three-wire Inverter Based on Interleaved Boost Converter

Tsair-Rong Chen, Yu-Lin Juan,* Hsu-Ting Liu, Chun-Ming Chen, and Yu-Tzu Lee

National Changhua University of Education, No. 2, Shi-Da Road, Changhua City 500, Taiwan

A high-voltage step-up ratio inverter for applications using batteries as the input power source is proposed to supply the emergency power requirement from a battery pack when the grid is down. The proposed inverter is composed of an interleaved coupled-inductor boost converter and a three-leg full-bridge inverter. Four series-connected lead acid batteries are used as the input power source. When 110 and 220 V AC outputs are required by the load sides at the same time, the 48 V DC input from the batteries would be boosted up to 350 V DC for the three-leg inverter to provide AC output power. However, if only 110 V AC is required, the proposed control strategy would reduce the step-up ratio for a lower DC link voltage of 175 V DC to enhance the conversion efficiency. Moreover, to minimize damage to the batteries, the interleaved circuit topology is adopted to reduce the input current ripple. A prototype with 400 W rated output power is finally constructed. The controller is implemented with a low-cost microcontroller, HT66F50. From the experimental results, it is seen that even under unbalanced load conditions, the output AC voltage is well controlled. The total efficiency of the proposed inverter with 110/220 V AC output is 89.8%, and the efficiency of the inverter with only 110 V AC output is 91.1%.

1. Introduction

To avoid power supply interruption in a remote area owing to natural disasters such as earthquake, typhoon, and debris flow, the emergency power supply system has attracted much attention in recent years. In the emergency power supply system, AC power of 110 and 220 V should be available for common electrical appliances and instruments. Gasoline/diesel engine generators or renewable energy sources are usually integrated into the power supply system. A battery pack is also required in the system for energy storage and buffer. In the most common system configuration, a 48 V battery pack with four series-connected batteries is used as the energy storage module. However, a DC input power with about 156 or 312 V is required for the conventional single-phase inverter to provide the 110 or 220 V AC output power, respectively.[1–4] Therefore, a step-up DC converter would be required to boost the 48 V DC power up to at least 156 or 312 V. Compared with the conventional boost converter, the coupled-inductor boost

converter could more easily provide a high-voltage step-up ratio.[5–10] However, the resulting current ripple in the low-voltage side would become higher than that in conventional topology, which would also result in additional power losses.

In this study, a high-voltage step-up ratio single-phase three-wire inverter is developed. A common 48 V battery pack is used as the input source in the proposed inverter. A two-phase coupled-inductor boost converter and a six-switch inverter are integrated into the proposed topology. The interleaved coupled-inductor boost converter would firstly convert the 48 V DC power into 175 or 350 V DC power for the six-switch inverter to properly provide 110 and 220 V AC output power for the AC side load requirement. By adopting the interleaved circuit topology, the input current ripple can therefore be reduced. Moreover, the conduction power losses can also be reduced owing to the power sharing in the two-phase topology.[11–14] As to the inverter, the sinusoidal pulse width modulation (PWM) mode is used to control the output AC voltage with 110 and 220 V rms. According to the loading demand, the output power can switch into only 110 or 110/220 V modes. A low-cost microcontroller unit, HT66F50, is used to realize the digital controller. The corresponding voltage and current signals are fed back to the microcontroller unit to control the DC link voltage as well as the output AC voltages.

2.   Circuit Topology and Operation Principles

The configuration of the proposed inverter is shown in Fig. 1. A two-phase coupled-inductor boost converter and a six-switch inverter are integrated into the proposed inverter. By using the coupled inductor, the voltage step-up ratio of the boost converter can be enhanced. Moreover, the conversion efficiency can be enhanced by sharing the power with the adopted two-phase interleaved circuit topology. The 48 V DC voltage of the battery pack would therefore easily be boosted up to the required voltage level for the six-switch inverter. The high-side and low-side switches in one arm of the six-switch inverter are driven by a set of complementary PWM signals. For a single-phase three-wire AC output application, the output terminal V shown in Fig. 1 is controlled as the neutral line. The line voltages for loads Z_1 and Z_2 are regulated to AC 110 V rms by adjusting the modulation index of the PWM gating signals of the switches S_{UH}, S_{WH}, S_{UL}, and S_{WL}.
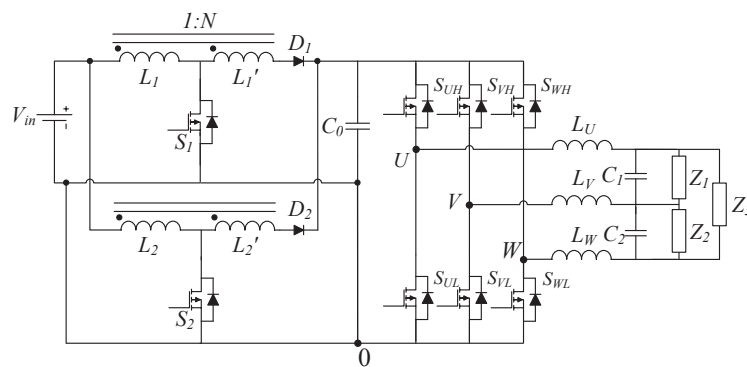

Fig. 1.   Circuit configuration of the proposed inverter.

The interleaved coupled-inductor boost converter is composed of two parallel-connected coupled-inductor boost converters as shown in Fig. 1. A set of gating signals with 180 degrees phase-shifted shown in Fig. 2 are used to control the two switches S_1 and S_2. The duty ratio of switches S_1 and S_2 are d_1 and d_2, respectively. It can be seen that the phase of the inductor current i_{L1} is also 180 degrees shifted with respect to that of the inductor current i_{L2}. The output current of the battery pack noted as the total input current i_{in} is the summation of the two inductor currents. Therefore, the current ripple of the battery pack output current would be reduced. As shown in Fig. 2, the i_{L1m} and i_{L2m} are the magnetizing currents of the coupled inductors L_1 and L_2, respectively. A lower current ripple would minimize damage to the battery pack as well.

The corresponding operation modes of the interleaved DC converter are shown in Fig. 3 and the operation principle in each mode is also described as follows.

- Mode 1 ($t_0 \leq t < t_1$): Both switches S_1 and S_2 are turned on. The stored energy in the inductors L_1 and L_2 are increased by the input DC power source. The energy stored in the DC link capacitor C_0 is released to the second-stage inverter.

- Mode 2 ($t_1 \leq t < t_2$): The switch S_1 is still turned on in this mode and the switch S_2 is turned off. The diode D_2 is then turned on for releasing the energy from the inductor L_2 to the DC link. The equivalent model of the coupled inductor is shown in Fig. 4. It is seen that the
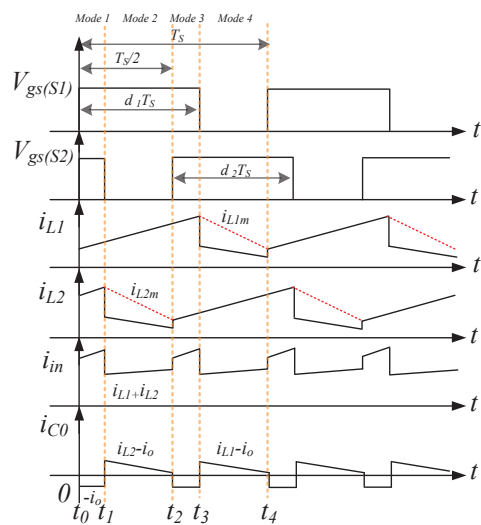

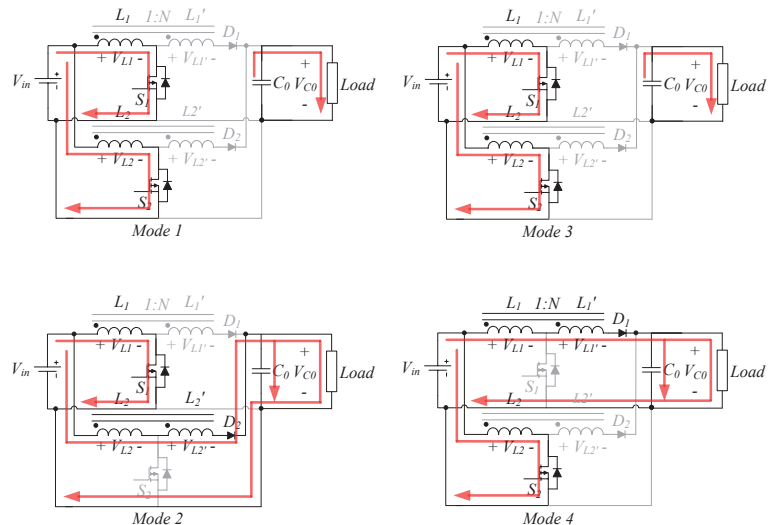Fig. 2. (Color online) Relative waveforms of the interleaved boost converter.

Fig. 3. (Color online) Operation modes of the interleaved-coupled inductor boost converter.
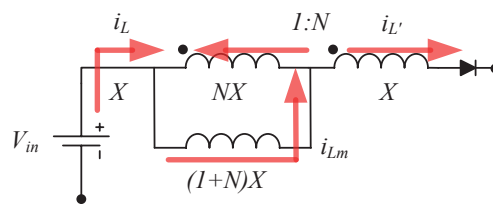

Fig. 4. (Color online) Equivalent model of the coupled inductor.

current through diode D_2 would be expressed as $i_{L2m} \times [1/(N+1)]$, where N is the turn ratio.

- Mode 3 ($t_2 \leq t < t_3$): In this mode, the switch S_2 would be turned on again. Therefore, the operation principle of this mode is similar to that of mode 1.
- Mode 4 ($t_3 \leq t < t_4$): The switch S_1 is turned off in this mode, then diode D_1 would be turned on to release the energy from the inductor L_1 to the DC link. The currents in the coupled inductor L_1 are similar to those in the coupled inductor L_2 in mode 2. The current of D_1 would be $i_{L1m} \times [1/(N+1)]$.

To ensure that the converter is operated under continuous conduction mode, the secondary side current of each coupled inductor should not be reduced to zero. As shown in Fig. 5, the design criteria of the inductor can then be derived as Eqs. (1) to (4). Moreover, the peak value of each phase input current can also be derived as Eq. (5).

$$\frac{1}{2}(\Delta i_{L'} + 2a)(1-D)T_S = \frac{V_o}{2R_L}T_S \tag{1}$$

$$\Delta i_{L'} = \frac{di_{L2'}}{dt}(1-D)T_S \tag{2}$$

$$a = \frac{V_o}{2(1-D)R_L} + \frac{V_{in}-V_o}{2(N+1)^2 L}(1-D)T_S \tag{3}$$

$$L_{1,2} \geq \frac{(V_o - V_{in})(1-D)^2 R_L T_S}{(N+1)^2 V_o} \tag{4}$$

$$i_{Lp} = i_{Lmp} = (N+1)\left[\frac{V_o}{2(1-D)R_L} + \frac{(V_o - V_{in})(1-D)T_S}{2(N+1)^2 L}\right] \tag{5}$$

As to the six-switch inverter, there are two operation modes proposed in this study according to the AC side load requirement. While the AC 220 V rms output power is required, the six-switch inverter would be operated in mode A. Otherwise, when only 110 V rms is demanded at the load terminals, the six-switch inverter would be operated in mode B to reduce the DC link voltage. Hence, the voltage step-ratio requirement of the interleaved coupled-inductor boost converter can be reduced to enhance the conversion efficiency.[15] The PWM profiles for the proposed two operation modes are shown in Fig. 6 and the corresponding principles are described as follows.
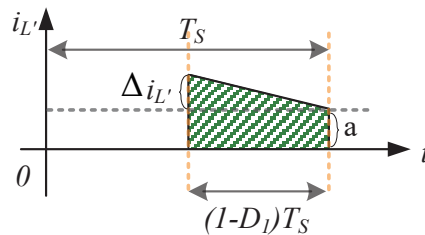

Fig. 5.　(Color online) Current of the diode in the boost converter.
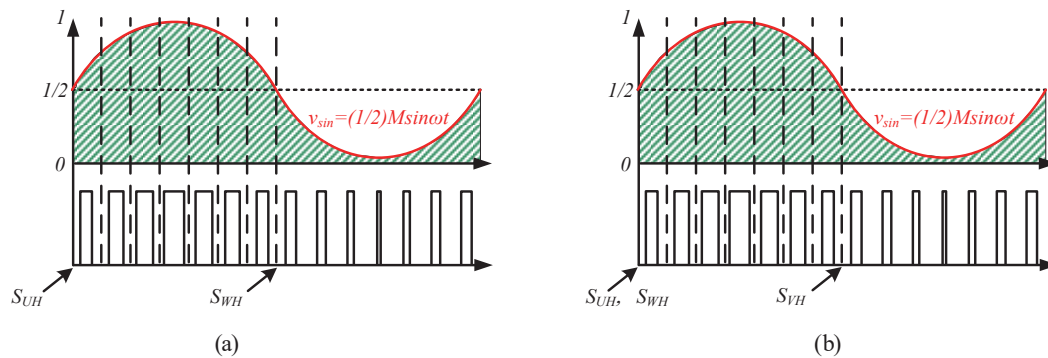
Fig. 6.   (Color online) Switching patterns in operation (a) mode A and (b) mode B.

- Mode A:

   In this mode, the DC link voltage is boosted up to 350 V for the six-switch inverter to generate 220 and 110 V rms AC voltage at the load sides. The phase V is controlled to be the neutral line of the single-phase three-wire 110/220 V AC output application. The two legs (S_{UH}, S_{UL} and S_{WH}, S_{WL}) are controlled by a set of sinusoidal PWM signals with a phase difference of 180 degrees as shown in Fig. 6(a). It is seen that the control signal of S_{WH} is 180 degrees lagged with respect to that of S_{UH}. Two switches on the same leg are switched by a set of complementary gating signals.

- Mode B:

   In this mode, there is only 110 V AC voltage required at the load sides. The switching patterns for the arms are shown in Fig. 6(b). The phase V controlled by switches S_{VH} and S_{VL} is no longer controlled to be the neutral line. The switches S_{UH} and S_{WH} are controlled by the same PWM signal, and the control signal of S_{VH} is 180 degrees lagged with respect to that of S_{UH} and S_{WH} in this mode. Therefore, there would be two 110 V AC outputs of V_{UV} and V_{VW} with 180 degrees phase difference. As a result, the DC link voltage is only boosted up to 175 V.

3.   Controller Diagram of Proposed Inverter

   There are two control objectives in operating the proposed inverter. Firstly, according to the load demand at the AC output terminals, the DC link voltage would be regulated to 350 or 175 V with respect to the operation mode A or mode B. The DC link voltage and two inductor currents of the two-phase boost converter are sensed and fed back to the microcontroller unit as shown in Fig. 7. Secondly, the sinusoidal PWM signals in the corresponding operation modes illustrated in Sect. 2 would be generated by the microcontroller unit to control the six switches in the three-arm inverter. The corresponding control block diagrams of mode A and mode B are shown in Figs. 8 and 9, respectively.

   As shown in Fig. 7, the DC link voltage of the capacitor C_0 is denoted as V_{C0} and the inductor currents of inductors L_1 and L_2 are denoted as I_{L1} and I_{L2}, respectively. The command of the total input current, namely, $I_{L\_command}$, is obtained from the PI controller in the voltage control loop. The command of the DC link voltage $V_{C0}{}^*$ is set to 350 V for operation mode A or 175 V for mode B. Then, the current command for each inductor current in the two-phase converter is
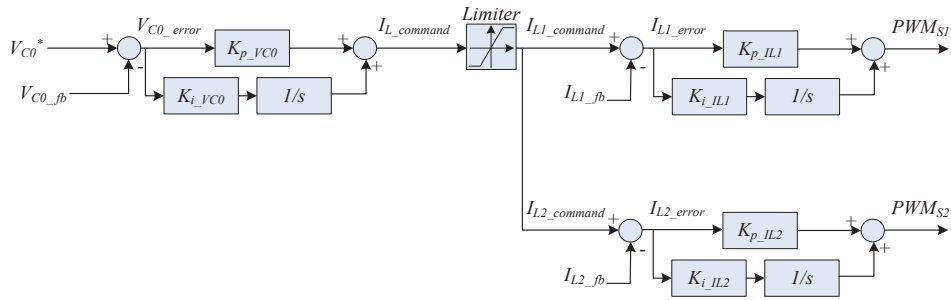
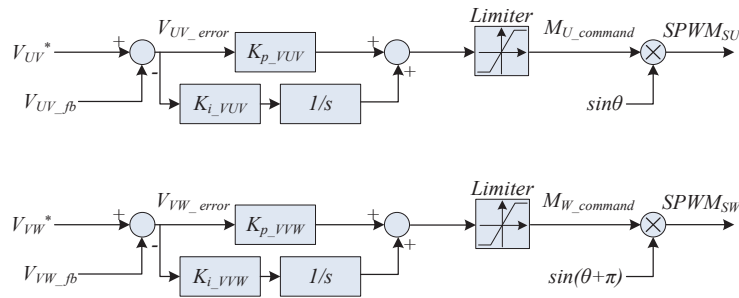Fig. 7.   (Color online) Control block diagram of the interleaved boost converter.

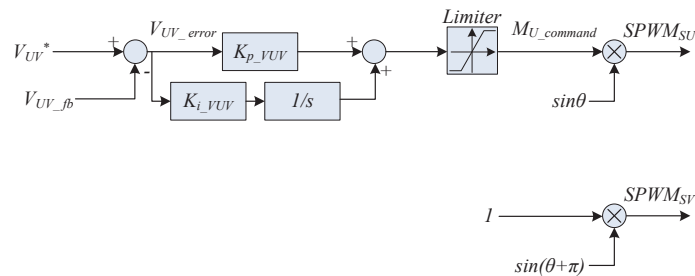Fig. 8.   (Color online) Control block diagram of operation mode A.

Fig. 9.   (Color online) Control block diagram of operation mode B.

equal to the command $I_{L\_command}$ for sharing the power flow. As a result, the PWM signals for switches S_1 and S_2 would be generated accordingly.

For the control block diagram for operation mode A as shown in Fig. 8 , the line voltage V_{UV} for load Z_1 would be 110 V rms and 180 degrees phase-shifted with respect to the line voltage V_{VW} for load Z_2. Therefore, the line voltage V_{UW} for load Z_3 would be 220 V rms, which is the summation of V_{UV} and V_{VW}. It can be seen that the phase difference between the modulation indexes of the PWM signals for switches S_{UH} and S_{WH} is 180 degrees. The PWM signals of switches S_{UL} and S_{WL} are complementary to that of switches S_{UH} and S_{WH}, respectively. The

peak values of the two AC output voltages are fed back and denoted as V_{UV_fb} and V_{VW_fb}. Then, the corresponding modulation index required for the amplitude control of each AC output voltage would be calculated using the proportion–integration (PI) controller. In this mode, the output terminal V should be the controller to be the neutral node. Hence, a set of complementary PWM signals with 50% duty ratio are used to control switches S_{VH} and S_{VL}.

Figure 9 shows the control block diagram of mode B. The modulation indexes for switches S_{UH} and S_{WH} are in phase to each other. A sinusoidal PWM signal with 180 degrees phase lag is adopted to control the switch S_{VH} in this mode. As a result, only two 110 V rms voltages would be provided at the output terminals and the required DC link voltage would be twice lower than that in mode A. The step-up ratio of the converter can therefore be reduced to enhance the conversion efficiency.

4. Experimental Results

Figure 10 shows the constructed prototype of the proposed high-voltage step-up ratio single-phase three-wire inverter. The corresponding circuit parameters of the constructed hardware are shown in Table 1. Figure 11 shows the measured waveforms of the control signals of
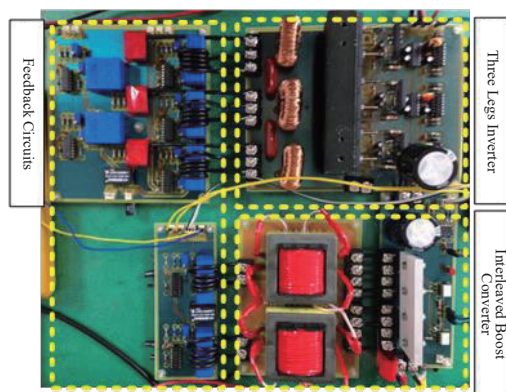

Fig. 10. (Color online) Constructed prototype of proposed inverter.
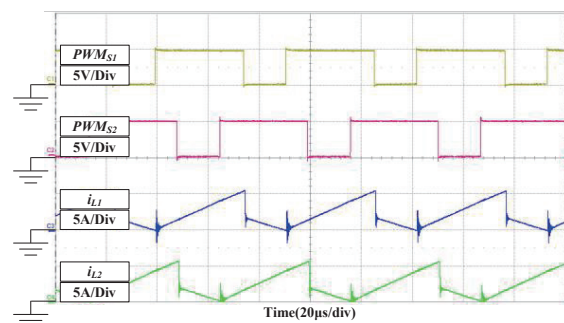

Fig. 11. (Color online) Relative input waveforms of the proposed inverter.

Table 1
Circuit parameters.

Rated power	400 W
Lead-acid batteries	12 V/22AH
Switching frequency	19.53 kHz
Primary side inductor L_1, L_2	300 μH
Secondary side inductor L_1', L_2'	1200 μH
DC link capacitor C_0	470 μF/400 V
DC link voltage	350/175 V
AC output inductor L_U, L_V, L_W	2 mH
AC output capacitor C_1, C_2	6.6 μF
Output AC voltage	110/220 V

switches S_1 and S_2 and the inductor currents i_{L1} and i_{L2}. The control signals of switches S_1 and S_2 are interleaved by 180 degrees. The total input current from the battery tank is shown in Fig. 12. It can be seen that the ripple on the input current is greatly reduced. The input voltage 48 V DC is boosted up to 350 V while providing 400 W power to the DC link, where I_o is the output current to the DC link. The reduced current ripple on the battery output current would also reduce the loss caused by the equivalent resistance in the battery and prevent additional damage to the battery.

The efficiency comparison between the adopted two-phase interleaved boost converter and the conventional single-phase boost converter with 400 W rated output power is shown in Fig. 13. In the operation under light to half load, the efficiency of the interleaved converter is about 3% higher. As to the heavy load condition, the interleaved topology can provide even higher efficiency of about 4%, which is because of the higher conduction losses in the single-phase boost converter.

Figure 14 shows the output waveforms while the inverter is operated under mode A as mentioned in the previous section. The inverter provided 50 W to load Z_1 and 350 W to load Z_2. It seems that there is no difference between the two output voltages on the loads Z_1 and Z_2, i.e., V_{UV} and V_{VW}. The results of the inverter operated under mode B are shown in Fig. 15. The total output is 400 W, which is 200 W for load Z_1 and 200 W for load Z_2. The total efficiency of the proposed inverter is shown in Fig. 16. It can be seen that the efficiency of the proposed topology would be better because the proposed controller can change the operation mode into
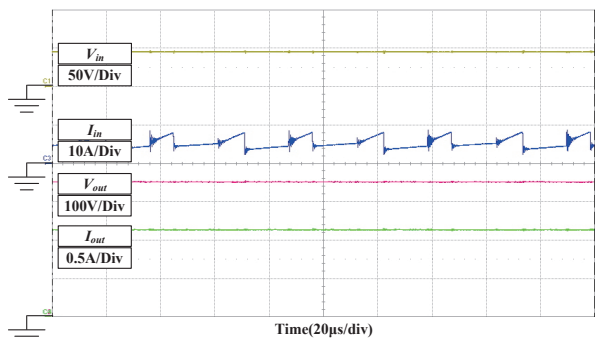

Fig. 12. (Color online) Waveforms of input voltage/ current and output voltage/current of the interleaved boost converter.
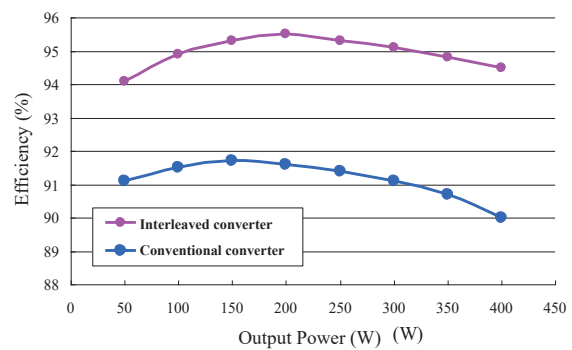

Fig. 13. (Color online) Efficiency comparison between interleaved and conventional converters.
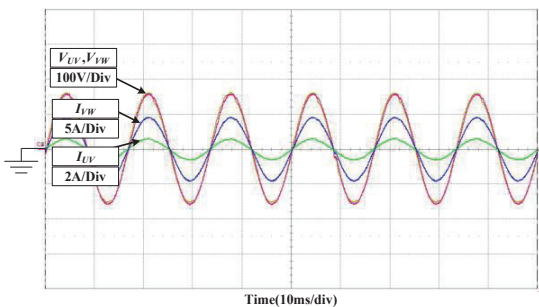

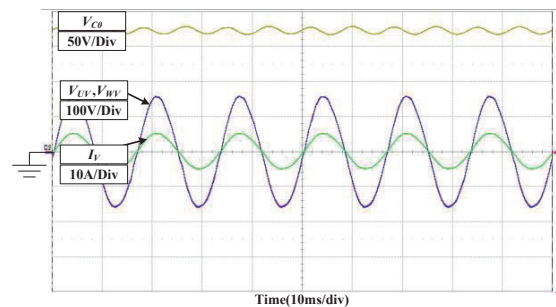Fig. 14. (Color online) Output waveforms of the inverter under operation mode A.

Fig. 15. (Color online) Output waveforms of the inverter under operation mode B.
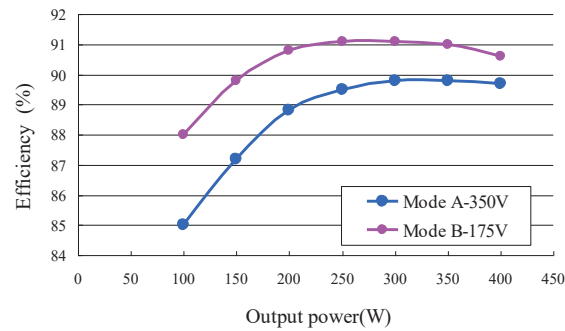
Fig. 16.   (Color online) Total efficiency of the proposed inverter in different modes.

mode B while there is only 110 V AC load demand, and the DC link is only required to be boosted up to 175 V DC.

5.   Conclusions

In this study, a high-voltage step-up ratio single-phase three-wire inverter is proposed for providing emergency power from a battery pack. By adopting the coupled inductor, the voltage step-up ratio was increased for boosting the battery pack terminal voltage to the required level. Furthermore, an additional control strategy for the inverter with only 110 V AC loading demand is proposed. In this operation mode, the voltage step-up ratio would be only half of that in the normal operation mode with 110 and 220 V output power. The lower voltage step-up ratio would therefore increase the conversion efficiency. From the experimental results, the proposed inverter can provide good efficiency higher than 90% and up to about 91.6% while only 110 V AC is required at the load side. The efficiency can also remain up to about 89.8% while the 220 V AC is required. The experiments with unbalanced load between two output AC ports are also carried out to verify that the proposed inverter can still provide stable 110 and 220 V AC output power.

References

1   X. Zhang, L. Jiang, J. Deng, S. Li, and Z. Chen: IEEE Trans. Power Electron. **8** (2014) 4270.
2   T. Tanaka, T. Sekiya, H. Tanaka, M. Okamoto, and E. Hiraki: IEEE Trans. Ind. Appl. **6** (2013) 2628.
3   J. Loncarski, M. Leijon, M. Srndovic, C. Rossi, and G. Grandi: Energies **5** (2015) 3832.
4   F. J. Lin, H. C. Chiang, and J. K. Chang: Energies **12** (2016) 993.
5   S. M. Chen, T. J. Liang, L. S. Yang, and J. F. Chen: IEEE Trans. Power Electron. **4** (2012) 1809.
6   Y. Zhao, W. Li, and X. He: IEEE Trans. Power Electron. **6** (2012) 2869.
7   J. M. Shen, H. L. Jou, and J. C. Wu: IET Power Electron. **9** (2012) 1847.
8   L. Y. Chang, J. H. Chang, K. H. Chao, and Y. N. Chung: Energies **10** (2016) 792.
9   Y. T. Chen, W. C. Lin, and R. H. Liang: Int. J. Circuit Theory Appl. **43** (2014) 967.
10 T. V. Nguyen, P. Petit, M. Aillerie, C. Salame, and J. P. Charles: Int. J. Circuit Theory Appl. **43** (2014) 1042.
11 W. Li, X. He, D. Xu, and B. Wu: IEEE Trans. Ind. Electron. **3** (2012) 1650.

12 W. Li, X. Xiang, C. Li, W. Li, and X. He: IEEE Trans. Power Electron. **1** (2013) 300.
13 B. C. Barry, J. G. Hayes, and M. S. Ryłko: IEEE Trans. Power Electron. **12** (2015) 6551.
14 C. L. Shen, P. C. Chiu, and Y. C. Lee: Energies **11** (2016) 871.
15 R. W. Erickson and D. Maksimovic: Fundamentals of Power Electronics (Springer, New York, 2000) 2nd ed.

About the Authors

Tsair-Rong Chen was born in Taichung, Taiwan, R.O.C., in 1956. He graduated in 1986 from National Chen Kung University, Taiwan, with a B.S. degree and in 1988 with an M. S. degree, majoring in electrical engineering. Afterward, he attended National Sun Yat-sen University, Taiwan, to receive a Ph.D. degree in 1991 majoring in electrical engineering. He is a distinguished professor in the Department of Electrical Engineering, National Changhua University of Education, Taiwan.

Yu-Lin Juan was born in Kaohsiung, Taiwan, R.O.C., in 1979. He graduated in 2001 from National Chen Kung University, Taiwan, with a B.S. degree in electrical engineering. Afterward, he attended National Tsing Hua University, Taiwan, to receive an M.S. degree in 2003 and a Ph.D. degree in 2010, majoring in electrical engineering. He is an associate professor in the Department of Electrical Engineering, National Changhua University of Education, Taiwan.

Hsu-Ting Liu was born in Changhua, Taiwan, R.O.C., in 1966. She graduated in 2013 from National Changhua University of Education, Taiwan, with an M.S. degree in electrical engineering. Currently, she is a Ph.D. student of the Department of Electrical Engineering, National Changhua University of Education, Taiwan.

Chun-Ming Chen was born in Taichung, Taiwan, R.O.C., in 1963. He majored in electrical engineering and graduated in 1989 from National Taipei Industrial College. With enthusiasm and work experience at power stations, he started studying in National Changhua University of Education, Taiwan to receive an M.S. degree in 2009 and kept on studying for a Ph.D. degree majoring in electrical engineering. He had work experience in Gibsin Engineers Ltd., and his professional experience is on the construction of traditional power stations as well as wind farms and solar farms.

Yu-Tzu Lee was born in Changhua, Taiwan, R.O.C., in 1970. She started studying in National Changhua University of Education, Taiwan, to receive an M.S. degree in 2013 and kept on studying for a Ph.D. degree majoring in electrical engineering. She had work experience in a cram school, and her research interests are in education and radio frequency identifier (RFID) applications.